A rapid approach to lipid profiling of mycobacteria using 2D HSQC NMR maps

Engy A. Mahrous, Robin B. Lee, and Richard E. Lee[1]

Department of Pharmaceutical Sciences, University of Tennessee Health Science Center, Memphis, TN 38163

Abstract **Mycobacteria, including *Mycobacterium tuberculosis*, are characterized by a unique cell wall rich in complex lipids, glycolipids, polyketides, and terpenoids. Many of these metabolites have been shown to play important roles in mycobacterial virulence and their inherent resistance to many antibiotics. Here, we report the development of a new simple method for global analysis of these metabolites using two-dimensional ^{1}H-^{13}C heteronuclear single quantum coherence nuclear magnetic resonance. The major advantages of this method are as follows: the small amount of sample and the minimal sample manipulation required; a relatively short procedural time; and the ability to rapidly attain a qualitative and quantitative lipid profile of a mycobacterial sample in which the majority of the clinically relevant lipids can be observed simultaneously. The effectiveness of this method is demonstrated in four different areas of major concern to the mycobacterial research community: *i*) adaptive changes in cell wall lipids as a result of drug treatment; *ii*) analysis of gene function; *iii*) characterization of new mycobacterial species; and *iv*) analysis of the production of virulence factors in clinical isolates of *M. tuberculosis*. This method is complementary to mass spectrometry-based lipidomic technologies and provides an urgently needed tool to gain a better understanding of the role of lipids in mycobacteria pathogenesis.**—Mahrous, E. A., R. B. Lee, and R. E. Lee. **A rapid approach to lipid profiling of mycobacteria using 2D HSQC NMR maps. *J. Lipid Res.* 2008.** 49: **455–463.**

Supplementary key words two-dimensional ^{1}H-^{13}C heteronuclear single quantum coherence nuclear magnetic resonance • lipidomics • phenolic glycolipids • tuberculosis

Mycobacterial infections are responsible for several devastating human diseases worldwide, including tuberculosis, leprosy, and Buruli ulcer. The mycobacterial cell wall is rich in complex lipids, including glycolipids, polyketides, and terpenoids, that have been shown to play important roles in mycobacterial virulence and pathogenesis (1–5). Because of this impenetrable lipid coat, treatment of *Mycobacterium tuberculosis* infections and other emerging mycobacterial pathogens has proven challenging. Recently, differences in the virulence among different mycobacterial species and even strains belonging to the same species have been attributed to the ability of these strains to produce certain lipid molecules, such as the sulfolipids, phenolic glycolipids (PGLs), phthiocerol dimycocerosates, and acyl trehaloses (3, 6–9).

Multiple investigators have contributed a great deal to our understanding of the lipids and carbohydrates associated with the unique mycobacterial cell wall (10, 11). This knowledge is the product of elegant but lengthy experimental procedures involving the extraction, fractionation, and structural determination of individual cell wall components. However, few methods have been developed to simultaneously qualitatively and quantitatively examine the components in the entire cellular lipid pool, thereby allowing rapid determination of the similarities and differences between samples. Application of five two-dimensional (2D) TLC systems of increasing polarity by Dobson et al. (12) in the 1980s allowed the first global analysis of mycobacterial lipids and has found wide application in this field. Recently, MS- and LC-MS-based methods have been applied (13, 14). Cox and coworkers (13) developed Fourier transform ion cyclotron resonance mass spectroscopy as a tool to study virulence-conferring lipids of *M. tuberculosis* from small samples. This proved to be a very sensitive method, which was able to detect mycobacterial lipids such as sulfolipid-1 and phthiocerol dimycoceroate in infected tissues in vivo. The most recent effort was reported by Shui et al. (14), who used LC-MS methodology to detect the relative production of anionic lipids such as mycolic acids in response to different growth conditions.

Methods that strive for global analysis of the lipid pool of mycobacteria all have their strengths, but they also have limitations. 2D TLC methods are limited by the length of the procedure, the presence of overlapping spots, poor staining of some species, and difficulties in quantification. Additionally, 2D TLC does not provide any structural

Manuscript received 1 October 2007 and in revised form 2 November 2007.

Published, JLR Papers in Press, November 2, 2007.
DOI 10.1194/jlr.M700440-JLR200

[1] To whom correspondence should be addressed.
e-mail: relee@utmem.edu

information that can identify new molecules or help explain a change in the migration of others. The limitations common to most MS-based lipidomic methods include the differing abilities of lipid species to form ions and hence varying signal intensity as well as ion-quenching phenomena, in which the signal from poor ionizing lipids is quenched by more easily ionized species suppressing the former signal, which requires the prior separation of lipid species for accurate quantitation or the use of specialized mass spectrometers. These factors result in a loss of sensitivity for many of the nonpolar lipid metabolites of tuberculosis bacilli. NMR-based lipid analysis methods are less sensitive than MS-based methods and are typically limited by overlapping signals in the ^{1}H NMR spectrum and the low natural abundance of ^{13}C. Considering the wide variety of lipids associated with mycobacteria and the unique properties of these lipids, we believe that no single technique can effectively study all of these lipids. Therefore, the development of complementary techniques is an important task so that when combined they may allow us to advance the important understanding of the role of lipids in the virulence and pathogenesis of mycobacteria.

Here, we report a new method for global analysis of the mycobacterial cell wall-associated lipid pool that uses 2D ^{1}H-^{13}C heteronuclear single quantum coherence (HSQC) NMR for the analysis of a crude lipid extract from ^{13}C-enriched cells. The use of HSQC NMR disperses signals into two dimensions, providing an information-rich 2D lipid profile map in which key unique biomarker peaks can be resolved and used to diagnose and quantitate the presence of certain lipid species. We further describe the successful use of this method for the study of the following: *i*) adaptive changes in the cell wall lipids as a result of drug treatment; *ii*) analysis of gene function; *iii*) characterization of new mycobacterial species; and *iv*) analysis of the production of the virulence factor PGL in two clinical isolates of *M. tuberculosis*.

MATERIALS AND METHODS

Reagents

The deuterated solvents $CDCl_3$, CD_3OD, and D_2O were purchased from Cambridge Isotope Laboratories (Cambridge, MA). Glycerol-$^{13}C_3$ and D-glucose-$^{13}C_6$ were purchased from Isotec-Sigma-Aldrich (Miamisburg, OH). Ethambutol was purchased from Sigma-Aldrich (St. Louis, MO).

Bacterial strains and growth conditions

Mycobacterial strains were grown in Middlebrook 7H9 supplemented with 0.05% Tween (Difco, Detroit, MI), 10% albumin dextrose supplement, and 0.2% glycerol. ^{13}C labeling was performed by the substitution of dextrose and glycerol in this medium with 0.2% U-$^{13}C_6$-glucose and 0.2% U-$^{13}C_3$-glycerol, respectively. Bacterial cultures (20 ml) were inoculated at an optical density at 600 nm (OD_{600}) of 0.05 and were maintained at 37°C with continuous shaking at 200 rpm until an OD_{600} of 0.6–0.8 was reached. This yielded an ~150–200 mg cell pellet (wet weight). The entire pellet was used for the extraction described below. *M. liflandii*, *M. ulcerans*, and *M. marinum* cells were grown at 31°C without shaking in 175 cm^2 tissue culture flasks.

Ethambutol treatment

M. smegmatis mc^2155 cells were inoculated at an OD_{600} of 0.005 in ^{13}C-labeled Middlebrook 7H9. The cells were grown under three experimental conditions: *i*) in the absence of ethambutol (control experiment); *ii*) at IC_{20} concentration (0.1 μg/ml ethambutol); and *iii*) at IC_{50} concentration (0.2 μg/ml ethambutol). The cells were harvested when the control culture reached an OD_{600} of ~0.7.

Total lipid extraction

The cells were harvested by centrifugation at 3,700 *g* for 10 min. The cell pellet was washed twice with 5 ml of D_2O, removing the aqueous wash in between by centrifugation and decantation. In a final washing step, 1 ml of D_2O was added to the cell pellets and cells were centrifuged at 21,000 *g* for 10 min. After careful removal of the remaining D_2O, the wet pellet was weighed and subsequently extracted with a 2:1 (v/v) mixture of $CDCl_3$ and

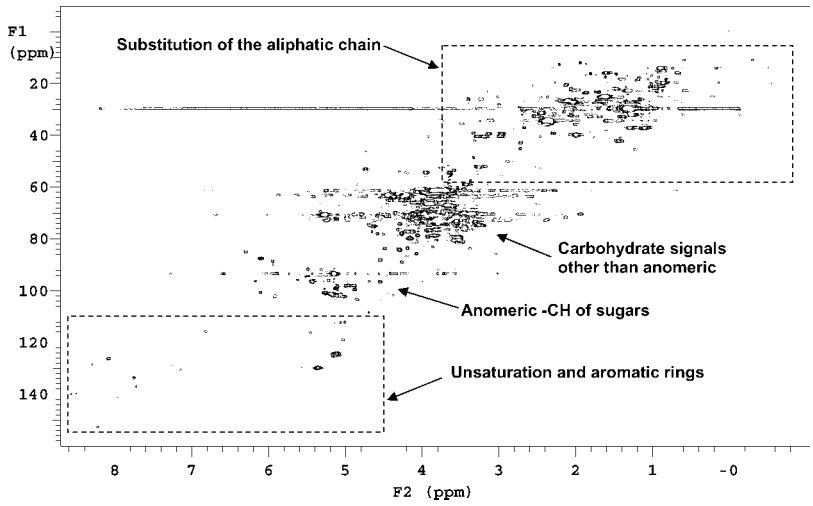

Fig. 1. ^{1}H-^{13}C heteronuclear single quantum coherence (HSQC) lipid profile of *M. tuberculosis* H37Rv. ^{1}H-^{13}C HSQC spectrum of the 2:1 (v/v) $CDCl_3/CD_3OD$ extract of *M. tuberculosis* H37Rv. The extract was obtained as described in the text. Total sample preparation time, including extraction, was 2 h. Total NMR acquisition time was 1 h, 40 min (number of increments = 256, number of transients = 10).

TABLE 1. $\delta^{1}H$ and $\delta^{13}C$ shifts for the unique biomarker signals of significant mycobacterial lipids

Lipid Molecule	δ ^{1}H (ppm)	δ ^{13}C (ppm)
Triacyl glycerol		
Glycerol		
C2	5.24	69
C1, C3	4.1, 4.28	61.9
Acyl group		
CH2(CO)	2.31	39.6
CH = CH	5.32	130.1
Acylated trehaloses		
Trehalose		
C1	5.05	94.3
C6 (Ac)	3.94, 4.65	64.2
C6 (Unac)	3.67, 3.8	61.6
Mycolic acid		
(CO) CH-	2.38	56.73
Cyclopropyl	−0.38	10.7
	0.2	13.3
Methoxy mycolate	4.46	56.2
	0.88, 1.26	44.9
Menaquinone[a,b]		
Ring protons H_a	8.1	125
	7.8	134
Isoprene side chain		
H_b	5.05	120
H_f	1.78	16.1
H_h	1.59	15.2
H_g	1.61	17.4
Mycobactins[a]		
Ring protons	6.86	116.9
	7.18	131.8
Phthicerol dimycocerosates		
Esterified phthiocerol	4.85	70.7
	0.95, 1.25	41.8
Mycocerosic acid		
	0.98	9.5
	0.85	12.7
	1.04	16.8
Phenolic glycolipids		
Ring protons	7.02	117.6
	7.14	129.7
Phe-glycopeptidolipids		
Aromatic protons	7.03	116.2
	7.18	129.6
α-CH	4.63	55
Phosphatidyl inositol mannoside[a,c]		
Mannose		
I-1	5.22	100.6
V-1	4.98	102.2
I-2	4.04	79.3
Inositol	4.73	72.2
	4.18	77.2
Mycolactone		
Macrolide ring		
	5.04	131.2
	2.02, 2.41	35.9
Side chain		
	7.92	143.1
	5.92	119.6

[a] Chemical shifts obtained from the literature and corrected to those observed when a 1:1 mixture of $CDCl_3$:CD_3OD is used for NMR acquisition.

[b] Letters correspond to the menaquinone substructures as described by Yamada et al (32).

[c] Roman numerals and Arabic numerals correspond to mannose residues and the positions of carbon atoms in the pyranose ring, respectively, as described by Gilleron et al (33).

CD_3OD (3 μl per milligram of cells). The extraction was performed at 37°C for 90 min with continuous shaking at 200 rpm. After extraction, CD_3OD (1 μl per milligram of cells) was added to allow the formation of a single solvent phase. The pellet was then separated by centrifugation, and the supernatant was transferred to a standard 5 mm NMR tube.

Sterility testing of extract

The sterility of the extract was tested by air-drying of the organic solvent under sterile conditions followed by suspension of the residue in 200 μl of sterile Middlebrook 7H9. The suspension was then used to inoculate Middlebrook 7H11 agar plates that were incubated at 37°C. No bacterial growth was observed after a period of 6 weeks. Sterility testing was performed in triplicate.

Isolation of PGL from *M. liflandii*

M. liflandii cells were grown to stationary phase in a 50 ml culture, harvested by centrifugation, and subsequently extracted with ethanol and concentrated in vacuo. The dried ethanolic extract of *M. liflandii* (80 mg) was resuspended in $CHCl_3$ and applied to a Biotage SP1 flash chromatography system equipped with a Biotage Si 12+M silica gel column that was eluted using a $CHCl_3$-to-$CHCl_3$/CH_3OD linear gradient of 9:1 (v/v). The major PGL was detected using silica TLC analysis of $CHCl_3$/CH_3OH (95:5, v/v) (Rf = 0.7) and visualized using cerric ammonium sulfate in 2 M sulfuric acid after charring. Fractions containing pure PGL were pooled and dried in vacuo.

NMR acquisition and data collection

The HSQC pulse sequence was applied using a 500MGHz Varian-INOVA NMR spectrometer equipped with a 5 mm triple resonance trpfg probe (Varian, Inc., Palo Alto, CA). HSQC spectra were acquired at 25°C for 256 increments and 12 scans per increment (~2 h). In investigating minor metabolites such as mycolactone, longer acquisition times were required to increase the intensity of the relatively weak signals (60–90 scans per increment). Other individual experimental parameters were optimized for each experiment. Signals were referenced to a tetramethylsilane internal standard. High-resolution magic angle spinning (HR-MAS) NMR was performed using a 4 mm gHX Nanoprobe (Varian). Experimental conditions for HR-MAS NMR were as described previously (15, 16).

RESULTS AND DISCUSSION

Because of the unusual complexity and diversity of the mycobacterial cell wall lipid pool, we chose to investigate a 2D NMR-based strategy to resolve signals for lipid species directly in a crude solvent extract without any separation. Application of a ^{1}H-^{13}C HSQC pulse sequence allows the user to overcome the broad overlapping peaks in a one-dimensional proton spectra by dispersing the signals into the second ^{13}C dimension. By using 2D HSQC NMR, it was hoped that qualitative and quantitative lipid profiles could be obtained for mycobacterial samples so that the majority of the clinically relevant lipids could be observed simultaneously. Additionally, it was expected that the use of NMR would be less likely affected by external factors such as ionization potential and relative polarity, which may introduce artifacts in other analytical methods used in lipidomic studies.

M. tuberculosis H37Rv was grown, harvested, and extracted as described in Materials and Methods, and the extract was analyzed by 2D HSQC NMR. Replacement of the carbon source in the growth medium with a universally labeled ^{13}C source (a mixture of U-$^{13}C_6$-glucose and U-$^{13}C_3$-glycerol) resulted in sufficient ^{13}C enrichment of the cell metabolites to enable us to obtain complex lipid maps within 2 h from a 20 ml Middlebrook 7H9 mycobacterial culture or from a lawn of mycobacteria grown on one 100 mm Middlebrook 7H11 agar plate. Such NMR lipid maps were not attainable from unlabeled cells using an increased concentration of crude lipid, as many species of lipid precipitate at higher concentrations. Signals in the HSQC spectrum were well dispersed and were categorized into three main regions: the most upfield region (δ^1H 0.5–3.0 ppm), representing the aliphatic chain of the lipid molecules; the far downfield region (δ^1H 5.2–8.5 ppm), representing unsaturated and aromatic substructures; and the middle region (δ^1H 3.2–5.4 ppm), which was crowded with signals, mainly from sugars attached to glycolipids (**Fig. 1**). Although there is significant crowding of many signal areas of the HSQC spectrum, because every molecule is represented by multiple signals, it was found that by careful analysis, at least one or two distinct signals for each lipid molecule of interest could be discovered within the spectra that did not overlap with other signals. These signals were designated as diagnostic biomarker signals, which can be used to define the presence or absence of a molecule of interest, and the peak intensity of these biomarker signals can also be integrated to determine the relative quantity of a certain molecule. The δ^1H and $\delta^{13}C$ shifts for the biomarker signals of many significant mycobacterial lipids were defined by comparison of the lipid profile with the chemical shifts of purified standards or values described in the literature. These values are reported in **Table 1**. These unique biomarker signals were then used to compare the lipid pools of different mycobacterial samples in subsequent experiments.

We believe that the most important application of this technique is as a rapid tool for the identification of qualitative or quantitative differences in molecules of interest that are involved in the virulence of mycobacteria. To demonstrate the utility of this technique in this area, we describe four types of experiments: *i*) definition of adap-

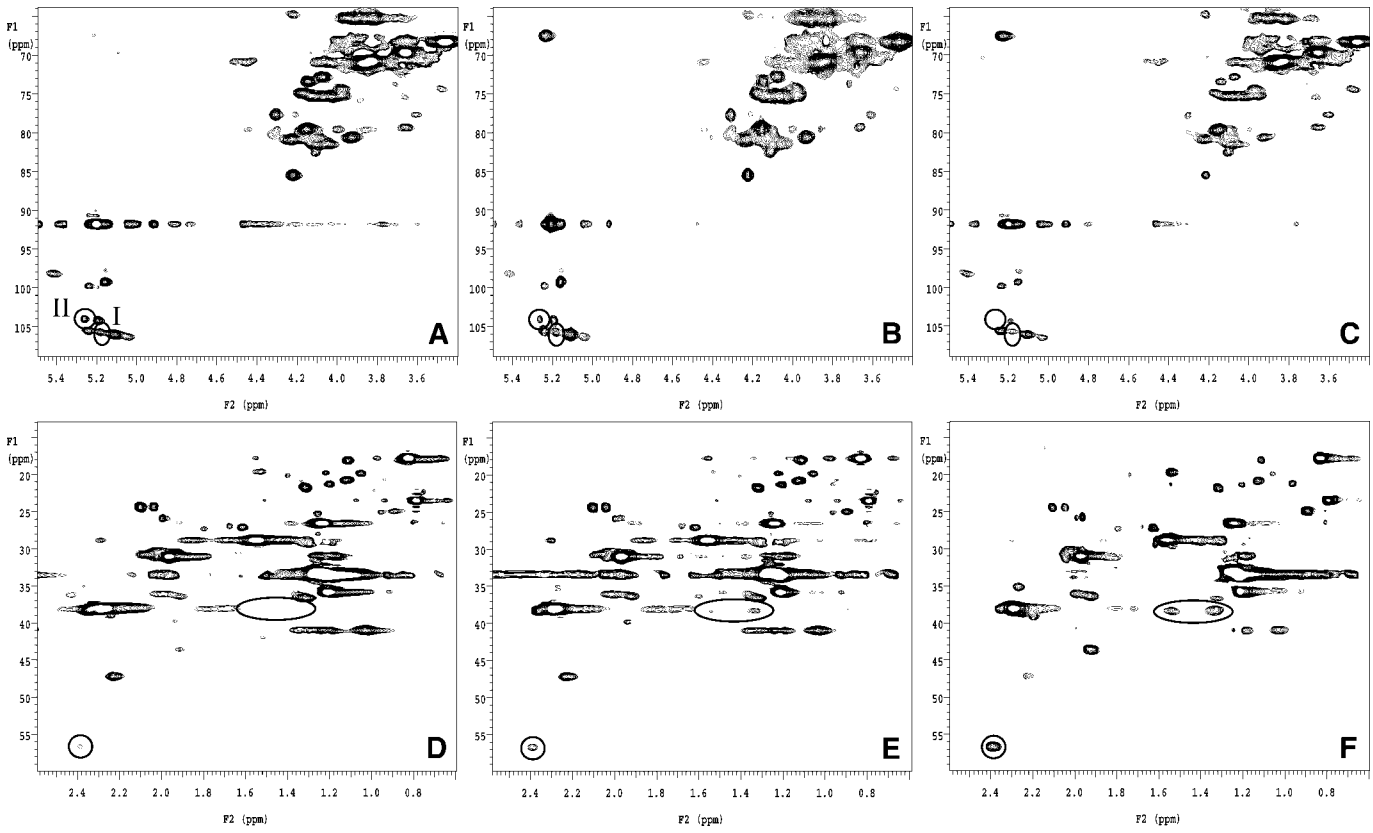

Fig. 2. Effect of ethambutol treatment on the cell wall of *M. smegmatis*. A–C: ^1H-^{13}C HSQC high-resolution magic angle spinning (HR-MAS) spectra (δ^1H 3.4–5.3 ppm, $\delta^{13}C$ 64–110 ppm) of live *M. smegmatis* cells (35 mg wet weight) in the absence of ethambutol (A), treated with ethambutol at 0.1 μg/ml (B), and treated with ethambutol at 0.2 μg/ml (C). All spectra were referenced to the anomeric signal of 6-β-Gal*f* (δ^1H 5.28 ppm, $\delta^{13}C$ 106.98 ppm). A gradual decrease in the intensity of signals corresponding to the branching of the Ara_6 motif of arabinogalactan, 3,5-α-Ara*f* (I), and 2-α-Ara*f*→3 (II) can be observed. D–F: ^1H-^{13}C HSQC spectra (δ^1H 0.6–2.6 ppm, $\delta^{13}C$ 13–60 ppm) of total lipid extract from *M. smegmatis* cells in the absence of ethambutol (D), treated with ethambutol at 0.1 μg/ml (E), and treated with ethambutol at 0.2 μg/ml (F). All spectra were referenced to the fatty acid terminal methyl signal (δ^1H 0.82 ppm, $\delta^{13}C$ 17.82 ppm). A gradual increase in the intensity of signals corresponding to trehalose mycolates can be observed (δ^1H 2.38 ppm, $\delta^{13}C$ 56.73 ppm and δ^1H 1.32 and1.54 ppm, $\delta^{13}C$ 38.17 ppm).

tive changes in the lipid profile as a result of drug treatment; *ii*) analysis of gene function; *iii*) characterization of species or strains; and *iv*) analysis of the production of virulence factors in clinical isolates of *M. tuberculosis*.

Definition of adaptive changes in the lipid profile as a result of drug treatment

The drug ethambutol was chosen to demonstrate the use of this technique to observe adaptive changes in lipid profiles as a result of drug treatment. Ethambutol is known to act by inhibition of the mycobacterial arabinosyltransferases EmbA–EmbC, particularly EmbB, which is required for the formation of the three arm branch of the 3,5-α-Ara*f* in the Ara_6 motif found in the cell wall arabinogalactan (17–19). Arabinogalactan is the main polysaccharide in the mycobacterial cell wall and is terminally substituted with mycolic acids that form the mycobacterial outer lipid membrane (1). Kilburn and Takayama (20) first reported that treatment with ethambutol results in the accumulation of trehalose monomycolates and dimycolates. *M. smegmatis* cells were treated with ethambutol at its IC_{20} and IC_{50} (0.1 μg/ml and 0.2 μg/ml, respectively). First, the production of a truncated form of arabinogalactan was validated using solid-state HR-MAS NMR on the live cell pellet as described previously (15). Then, the cellular lipids were extracted and the overall lipid profile was defined. Indeed, we were able to observe the gradual accumulation of trehalose mycolates in the lipid profiles of cells treated with increasing concentrations of ethambutol compared with control cells (**Fig. 2**). This ability to rapidly observe the adaptive response to drug treatment is an important application of this technique.

Analysis of gene function

To demonstrate the use of this technique to explore gene function, we studied the lipid pools of the mycolactone-producing mycobacterium *M. ulcerans*, with mutations in the mycolactone biosynthesis pathways. Mycolactone is the main virulence factor of *M. ulcerans*, the causative agent of Buruli ulcer and other closely related species (21–23). Three polyketide synthases have been shown to be involved in the biosynthesis of this polyketide-macrolide hybrid molecule

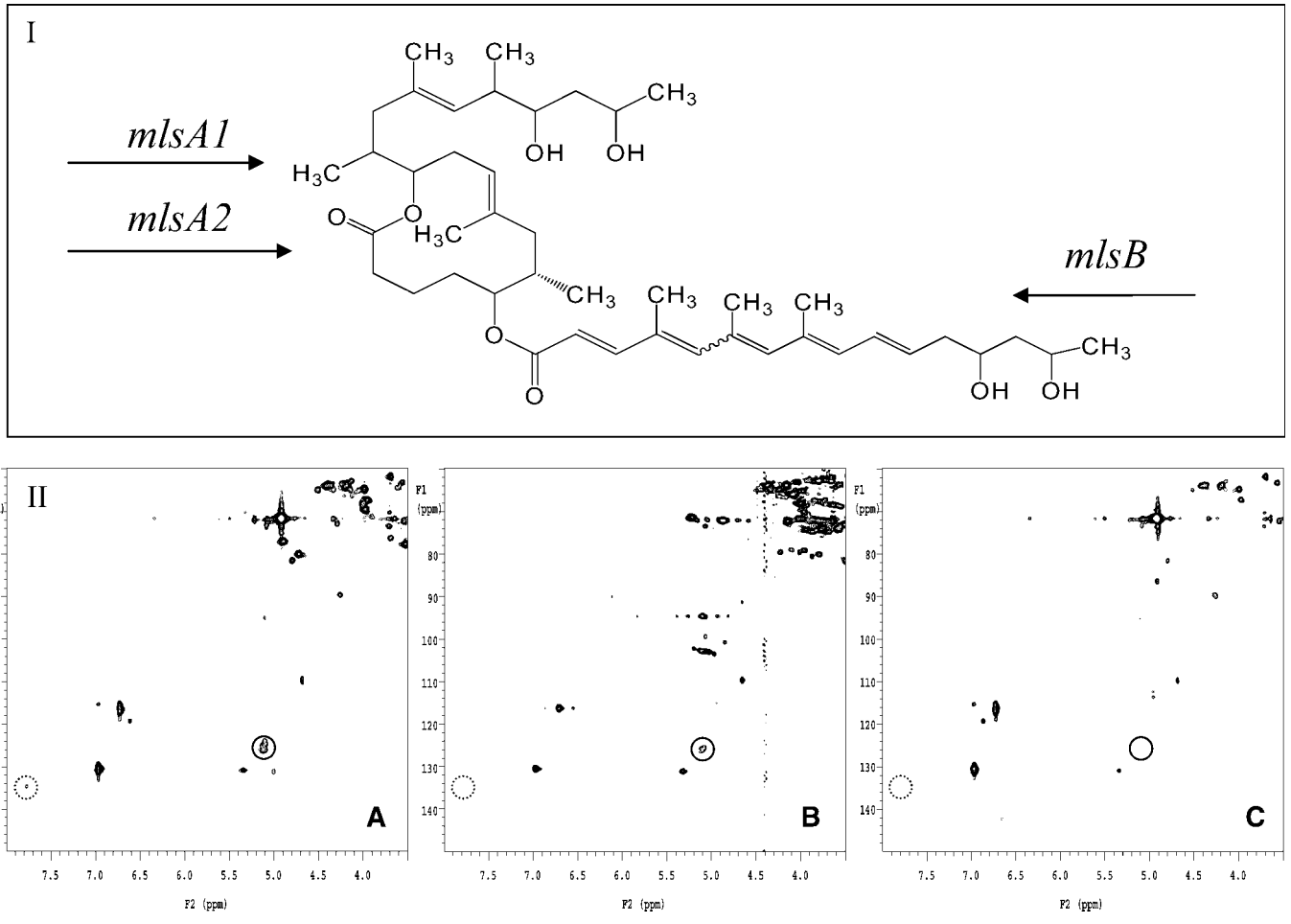

Fig. 3. Demonstration of gene function in different strains of *M. ulcerans*. Panel I: Structure of the macrolide toxin mycolactone. The roles of the three polyketide synthase enzymes that are involved in its biosynthesis are illustrated on the structure with solid arrows. Panel II: ^{1}H-^{13}C HSQC spectra ($\delta^{1}H$ 3.5–8.0 ppm, $\delta^{13}C$ 60–150 ppm) of total lipid extract from *M. ulcerans* 1615 (A), *M. ulcerans* 1615A (B), and *M. ulcerans* 1615::Tn104 (C). Signals representing the mycolactone core are circled with solid lines, and signals representing the side chain are circled with dashed lines.

(24). *mlsA1* and *mlsA2* are responsible for the biosynthesis of the core macrolide ring, whereas the biosynthesis of the polyene side chain is catalyzed by another polyketide synthase, *mlsB* (**Fig. 3**, upper panel). We compared the lipid profile of *M. ulcerans* 1615 (MU1615), which produces mycolactone A/B, with that of MU1615A, a mutant strain that is deficient in mycolactone biosynthesis (21). As expected, analysis of these profiles showed the total absence of mycolactone signals from the MU1615A strain. Signals corresponding to the core macrolide ring only were also detected in MU1615::Tn*104*, a genetically engineered strain that harbors an insertion in the *mlsB* gene, which therefore cannot produce the side chain but retains the ability to produce the macrolide core of mycolactone (Fig. 3, lower panel, a–c) (24). This experiment demonstrates the ability of this method to confirm gene function based on the changes observed in the lipid profile. Furthermore, it demonstrates the ability of this technique to be used to study metabolites of relatively low abundance, such as mycolactones.

Characterization of species or strains

To demonstrate the use of this method to characterize different species or strains, we studied the newly described species, *M. liflandii*, a frog pathogen that was first reported in 2004 (25). At that time, it was suggested that *M. liflandii* was closely related to either *M. marinum* or *M. ulcerans* (22). When the lipid profile of this species was compared with the profiles of other mycobacteria (*M. tuberculosis*, *M. smegmatis*, *M. ulcerans*, and *M. marinum*), indeed, the similarity between the *M. liflandii* lipid profile and those of *M. ulcerans* and *M. marinum* was very obvious (**Fig. 4A–**C). The *M. liflandii* lipid profile represented an intermediate lipid expression between *M. marinum*, which produces abundant glycolipids and carotenoids, and *M. ulcerans*, which lacks most of these molecules. This observation was validated recently through in-depth genomic study of several mycolactone-producing strains (26). That study suggested a recent reductive evolution of *M. ulcerans* from *M. marinum*, whereas other mycolactone-producing strains like *M. liflandii* were identified as an earlier divergence during this evolutionary process (26, 27). Another interesting finding from our study was that *M. liflandii* produces significant amounts of PGL, a class of lipids closely related to phthiocerol dimycocerosates, which are produced by some mycobacterial strains (28–30). Signals attributed to PGL from *M. liflandii* were found to

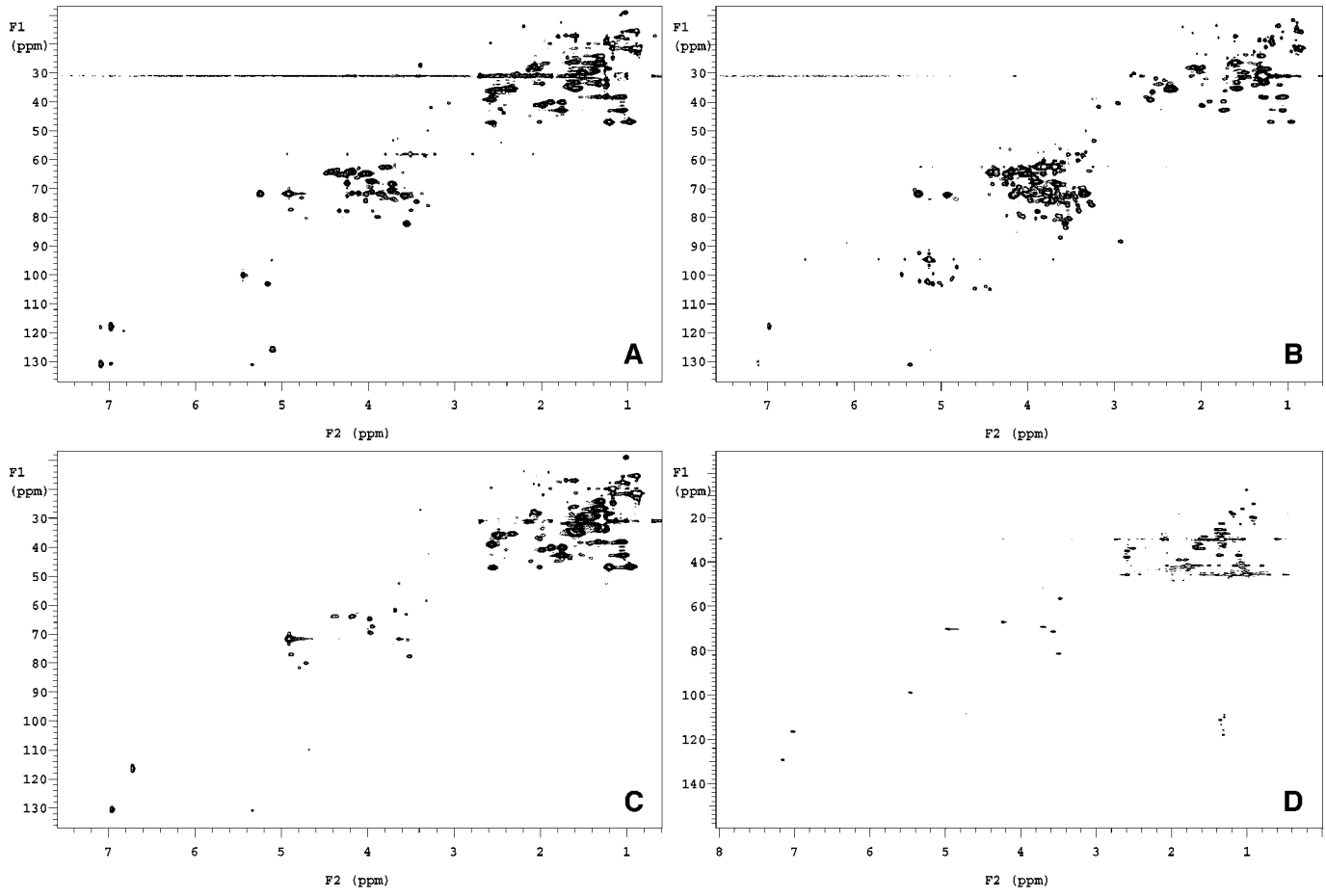

Fig. 4. Lipidomic characterization of *M. liflandii*. A–C: ^{1}H-^{13}C HSQC spectra (δ^{1}H 0.6–7.6 ppm, δ^{13}C 14–136 ppm) of total lipid extract from *M. liflandii* (A), *M. marinum* (B), and *M. ulcerans* (C). *M. liflandii* is thought to represent an intermediate stage in the reductive evolution of *M. ulcerans* from an *M. marinum* progenitor, which is reflected in these lipid profiles by comparing the diversity of the glycolipid pools of the three species. D: ^{1}H-^{13}C HSQC spectrum of the major phenolic glycolipid (PGL) purified from *M. liflandii* total lipid extract.

superimpose with signals corresponding to PGL in the *M. marinum* spectrum (31). This observation was confirmed by the subsequent isolation and structural characterization of this molecule, which was found to be phenolphthiodiolone glycosylated with 3-*O*-methyl-rhamnose at the phenolic hydroxyl (Fig. 4D).

Analysis of the production of virulence factors in clinical isolates of *M.tuberculosis*

To demonstrate the use of this technique to rapidly analyze the production of a specific virulence factor, we analyzed the lipid profiles of two well-known clinical isolates, the hypervirulent HN878 and the less virulent CDC1551, for differences in the production of the known virulence factor PGL. Recent studies have demonstrated that PGLs are produced in varying degrees by different clinical isolates of *M. tuberculosis* and that this may play a significant role in the hypervirulence of the Beijing/W lineage (6). A major obstacle in studying these molecules is their low abundance compared with other lipid molecules and the lack of a quick quantifiable test for their presence. This problem seemed like an excellent opportunity to apply this technique. The δ^1H and δ^{13}C chemical shifts defined for the isolated PGLs produced by *M. liflandii* described above were compared with the 2D HSQC spectra of the *M. tuberculosis* lipid profile. Three unoverlapping signals that are unique to PGL were identified, which can serve as excellent biomarkers for this metabolite. These three signals correspond to the benzylic protons (δ^1H 2.58, δ^{13}C 46.8 ppm) and the aromatic protons (δ^1H 7.02, δ^{13}C 117.6 ppm and δ^1H 7.29, δ^{13}C 130.05).

Because of differences in the glycosidation pattern between PGL molecules produced by *M. tuberculosis* and *M. liflandii*, a small difference in the chemical shift of the aromatic protons at the ortho-position to the glycosidic linkage was observed in their respective 2D HSQC spectra. The reported chemical shift for these protons in the PGL of *M. liflandii* were slightly upfield at δ^1H 7.14, δ^{13}C 129.7

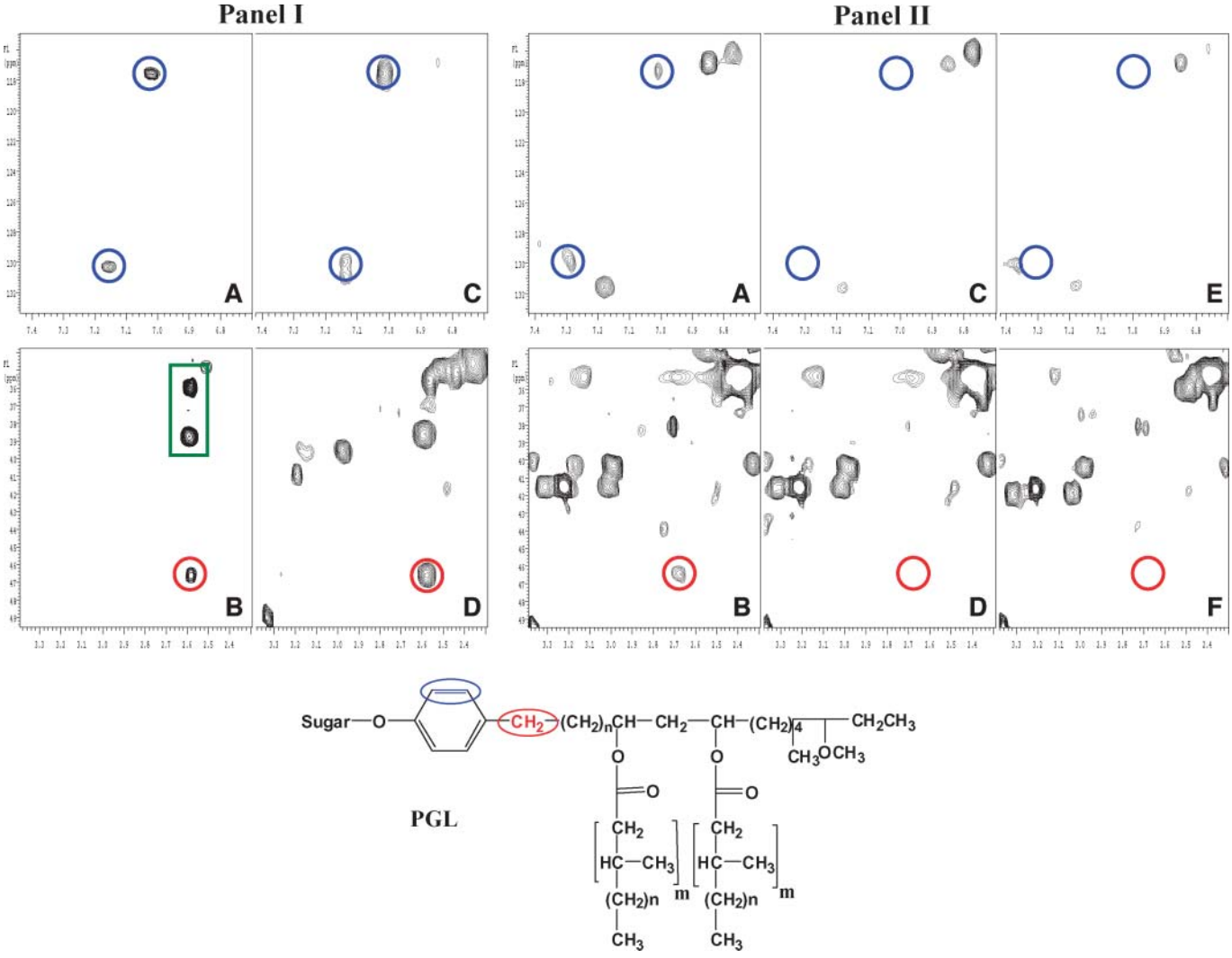

Fig. 5. Biomarkers for PGL and analysis of PGL in extracts from clinical isolates of *M. tuberculosis*. Panel I: *M. liflandii*. Purified PGL (A, B) and $CDCl_3$:CD_3OD cell extract (C, D). Panel II: *M. tuberculosis* cell extracts HN878 (A, B), HN878-Δ*pks* (C, D), and CDC1551 (E, F). Aromatic signals are circled in blue, and benzylic signals are circled in red. For simplicity, relevant smaller regions are shown from the whole HSQC spectra: A, C, and E (δH 6.7–7.4, δC 115–133); B, D, and F (δH 2.3–3.4, δC 33.8–49.4).

ppm, compared with δ^1H 7.29 and δ^{13}C 130.05 ppm in the PGL of *M. tuberculosis*. When the lipid profiles of two clinical isolates, the hypervirulent *M. tuberculosis* HN878 and the less virulent CDC1551, were compared (**Fig. 5**, panel II), these three biomarker signals were readily observable in the HN878 profile but were absent in the profiles of both CDC1551 and an HN878-Δ*pks* mutant in which the *pks 1-15* gene responsible for the production of PGL was effectively disrupted. The signal for the benzylic CH_2 in the HSQC spectra was found to have the same proton shift as that of the $CH_2\alpha$ to the carbonyl in the mycocerosate portion of this PGL (shown in green in Fig. 5, panel I, b). However, these benzylic protons possess a clear signal when dispersed in the ^{13}C dimension. This underscores the utility of the 2D HSQC approach to lipid profiling. It was noted also that it is often possible to use multiple biomarker peaks for the same molecule (phenolic and benzylic in this case), which adds greatly to the confidence in the results of this method.

Conclusions

In conclusion, we have developed a simple method to globally analyze mycobacterial cell wall lipids. This method allows for the simultaneous analysis of cell wall lipid species to pinpoint changes in the lipid profile as a result of gene mutation, drug treatment, or adaptation to environmental changes. Although this method does not have the fine sensitivity of MS-based lipidomic methods, it has the advantage of being suitable to analyze lipid species regardless of their polarity or ability to ionize and allows the simultaneous analysis of a broader range of lipids. This makes it a good complementary method for the lipidomic analysis of mycobacteria. Because of the rapid nature of this method, the simple procedures, and the small sample size required to produce a good quality spectrum using a standard high-field NMR spectrometer found in most research institutions, we expect that it will find wide application in studying mycobacterial lipid-mediated virulence and pathogenicity. Furthermore, we anticipate that the sensitivity of this technique could be improved by using low-volume probes to decrease the required sample size and using cryoprobe technology to improve signal-to-noise levels when studying molecules with lower abundance.

The authors thank Dr. Wei Li (University of Tennessee, Memphis) for technical assistance, Dr. Pamela L. C. Small (University of Tennessee, Knoxville) for kindly providing *M. ulcerans*, and *M. liflandii* strains, and Dr. Clifton Barry, 3rd (National Institutes of Health) for providing the *M. tuberculosis* HN878-Δ*pks* strain.

REFERENCES

1. McNeil, M. R., and P. J. Brennan. 1991. Structure, function and biogenesis of the cell envelope of mycobacteria in relation to bacterial physiology, pathogenesis and drug resistance: some thoughts and possibilities arising from recent structural information. *Res. Microbiol.* **142:** 451–463.
2. Laneelle, G., and M. Daffe. 1991. Mycobacterial cell wall and pathogenicity: a lipodologist's view. *Res. Microbiol.* **142:** 433–437.
3. Hunter, R. L., M. R. Olsen, C. Jagannath, and J. K. Actor. 2006. Multiple roles of cord factor in the pathogenesis of primary, secondary, and cavitary tuberculosis, including a revised description of the pathology of secondary disease. *Ann. Clin. Lab. Sci.* **36:** 371–386.
4. Dubnau, E., J. Chan, C. Raynaud, V. P. Mohan, M. A. Laneelle, K. Yu, A. Quemard, I. Smith, and M. Daffe. 2000. Oxygenated mycolic acids are necessary for virulence of *Mycobacterium tuberculosis* in mice. *Mol. Microbiol.* **36:** 630–637.
5. Onwueme, K. C., C. J. Vos, J. Zurita, J. A. Ferreras, and L. E. Quadri. 2005. The dimycocerosate ester polyketide virulence factors of mycobacteria. *Prog. Lipid Res.* **44:** 259–302.
6. Reed, M. B., P. Domenech, C. Manca, H. Su, A. K. Barczak, B. N. Kreiswirth, G. Kaplan, and C. E. Barry, 3rd. 2004. A glycolipid of hypervirulent tuberculosis strains that inhibits the innate immune response. *Nature.* **431:** 84–87.
7. De Voss, J. J., K. Rutter, B. G. Schroeder, H. Su, Y. Zhu, and C. E. Barry, 3rd. 2000. The salicylate-derived mycobactin siderophores of *Mycobacterium tuberculosis* are essential for growth in macrophages. *Proc. Natl. Acad. Sci. USA.* **97:** 1252–1257.
8. Cox, J. S., B. Chen, M. McNeil, and W. R. Jacobs, Jr. 1999. Complex lipid determines tissue-specific replication of *Mycobacterium tuberculosis* in mice. *Nature.* **402:** 79–83.
9. Pabst, M. J., J. M. Gross, J. P. Brozna, and M. B. Goren. 1988. Inhibition of macrophage priming by sulfatide from *Mycobacterium tuberculosis*. *J. Immunol.* **140:** 634–640.
10. Brennan, P. J. 2003. Structure, function, and biogenesis of the cell wall of *Mycobacterium tuberculosis*. *Tuberculosis (Edinb.).* **83:** 91–97.
11. Brennan, P. J., and H. Nikaido. 1995. The envelope of mycobacteria. *Annu. Rev. Biochem.* **64:** 29–63.
12. Dobson, G., D. E. Minnikin, S. M. Minnikin, M. Parlett, M. Goodfellow, M. Ridell, and M. Magnusson. 1985. Systematic analysis of complex mycobacterial lipids. *In* Chemical Methods in Bacterial Systematics. M. Goodfellow and D. E. Minnikin, editors. Academic Press, London. 237–265.
13. Jain, M., C. J. Petzold, M. W. Schelle, M. D. Leavell, J. D. Mougous, C. R. Bertozzi, J. A. Leary, and J. S. Cox. 2007. Lipidomics reveals control of *Mycobacterium tuberculosis* virulence lipids via metabolic coupling. *Proc. Natl. Acad. Sci. USA.* **104:** 5133–5138.
14. Shui, G., A. K. Bendt, K. Pethe, T. Dick, and M. R. Wenk. 2007. Sensitive profiling of chemically diverse bioactive lipids. *J. Lipid Res.* **48:** 1976–1984.
15. Lee, R. E., W. Li, D. Chatterjee, and R. E. Lee. 2005. Rapid structural characterization of the arabinogalactan and lipoarabinomannan in live mycobacterial cells using 2D and 3D HR-MAS NMR: structural changes in the arabinan due to ethambutol treatment and gene mutation are observed. *Glycobiology.* **15:** 139–151.
16. Li, W., R. E. Lee, R. E. Lee, and J. Li. 2005. Methods for acquisition and assignment of multidimensional high-resolution magic angle spinning NMR of whole cell bacteria. *Anal. Chem.* **77:** 5785–5792.
17. Escuyer, V. E., M. A. Lety, J. B. Torrelles, K. H. Khoo, J. B. Tang, C. D. Rithner, C. Frehel, M. R. McNeil, P. J. Brennan, and D. Chatterjee. 2001. The role of the *embA* and *embB* gene products in the biosynthesis of the terminal hexaarabinofuranosyl motif of *Mycobacterium smegmatis* arabinogalactan. *J. Biol. Chem.* **276:** 48854–48862.
18. Khoo, K. H., E. Douglas, P. Azadi, J. M. Inamine, G. S. Besra, K. Mikusova, P. J. Brennan, and D. Chatterjee. 1996. Truncated structural variants of lipoarabinomannan in ethambutol drug-resistant strains of *Mycobacterium smegmatis*. Inhibition of arabinan biosynthesis by ethambutol. *J. Biol. Chem.* **271:** 28682–28690.
19. Alderwick, L. J., M. Seidel, H. Sahm, G. S. Besra, and L. Eggeling. 2006. Identification of a novel arabinofuranosyltransferase (AftA) involved in cell wall arabinan biosynthesis in *Mycobacterium tuberculosis*. *J. Biol. Chem.* **281:** 15653–15661.
20. Kilburn, J. O., and K. Takayama. 1981. Effects of ethambutol on accumulation and secretion of trehalose mycolates and free mycolic acid in *Mycobacterium smegmatis*. *Antimicrob. Agents Chemother.* **20:** 401–404.
21. George, K. M., D. Chatterjee, G. Gunawardana, D. Welty, J. Hayman, R. Lee, and P. L. Small. 1999. Mycolactone: a polyketide toxin from *Mycobacterium ulcerans* required for virulence. *Science.* **283:** 854–857.
22. Mve-Obiang, A., R. E. Lee, E. S. Umstot, A. K. Trott, T. C. Grammer, J. M. Parker, B. S. Ranger, R. Grainger, E. A. Mahrous, and P. L. Small. 2005. A newly discovered mycobacterial pathogen isolated from laboratory colonies of Xenopus species with lethal infections produces a novel form of mycolactone, the *Mycobacterium ulcerans* macrolide toxin. *Infect. Immun.* **73:** 3307–3312.

23. Ranger, B. S., E. A. Mahrous, L. Mosi, S. Adusumilli, R. E. Lee, A. Colorni, M. Rhodes, and P. L. Small. 2006. Globally distributed mycobacterial fish pathogens produce a novel plasmid-encoded toxic macrolide, mycolactone F. *Infect. Immun.* **74:** 6037–6045.
24. Stinear, T. P., A. Mve-Obiang, P. L. Small, W. Frigui, M. J. Pryor, R. Brosch, G. A. Jenkin, P. D. Johnson, J. K. Davies, R. E. Lee, et al. 2004. Giant plasmid-encoded polyketide synthases produce the macrolide toxin of *Mycobacterium ulcerans*. *Proc. Natl. Acad. Sci. USA.* **101:** 1345–1349.
25. Trott, K. A., B. A. Stacy, B. D. Lifland, H. E. Diggs, R. M. Harland, M. K. Khokha, T. C. Grammer, and J. M. Parker. 2004. Characterization of a *Mycobacterium ulcerans*-like infection in a colony of African tropical clawed frogs (*Xenopus tropicalis*). *Comp. Med.* **54:** 309–317.
26. Stinear, T. P., T. Seemann, S. Pidot, W. Frigui, G. Reysset, T. Garnier, G. Meurice, D. Simon, C. Bouchier, L. Ma, et al. 2007. Reductive evolution and niche adaptation inferred from the genome of *Mycobacterium ulcerans*, the causative agent of Buruli ulcer. *Genome Res.* **17:** 192–200.
27. Yip, M. J., J. L. Porter, J. A. Fyfe, C. J. Lavender, F. Portaels, M. Rhodes, H. Kator, A. Colorni, G. A. Jenkin, and T. Stinear. 2007. Evolution of *Mycobacterium ulcerans* and other mycolactone-producing mycobacteria from a common *Mycobacterium marinum* progenitor. *J. Bacteriol.* **189:** 2021–2029.
28. Daffe, M., A. Varnerot, and V. V. Levy-Frebault. 1992. The phenolic mycoside of *Mycobacterium ulcerans*: structure and taxonomic implications. *J. Gen. Microbiol.* **138:** 131–137.
29. Riviere, M., J. J. Fournie, and G. Puzo. 1987. A novel mannose containing phenolic glycolipid from *Mycobacterium kansasii*. *J. Biol. Chem.* **262:** 14879–14884.
30. Chatterjee, D., C. M. Bozic, C. Knisley, S. N. Cho, and P. J. Brennan. 1989. Phenolic glycolipids of *Mycobacterium bovis:* new structures and synthesis of a corresponding seroreactive neoglycoprotein. *Infect. Immun.* **57:** 322–330.
31. Dobson, G., D. E. Minnikin, G. S. Besra, A. I. Mallet, and M. Magnusson. 1990. Characterisation of phenolic glycolipids from *Mycobacterium marinum*. *Biochim. Biophys. Acta.* **1042:** 176–181.
32. Yamada Y, Inouye G, Tahara Y, and Kondo K. 1976. On the chemical structure of menaquinones with the tetrahydrogenated isoprenoid side chain. *Biochim Biophys Acta.* **486:**195–203.
33. Gilleron M, Nigou J, Cahuzac B, Puzo G. 1999. Structural study of the lipomannans from Mycobacterium bovis BCG: characterisation of multiacylated forms of the phosphatidyl-myo-inositol anchor. *J Mol Biol.* 285:2147–2160.